SEMARAK ILMU PUBLISHING

Journal of Advanced Research in Fluid Mechanics and Thermal Sciences

Journal homepage:
https://semarakilmu.com.my/journals/index.php/fluid_mechanics_thermal_sciences/index
ISSN: 2289-7879

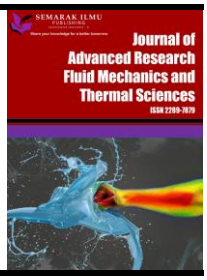

Impact on Casson Nanofluid Flow Across an Inclined, Slanted Surface by Radiation, Energy and Mass Transfer

Sumathi Mini Gopinathan[1], Prathi Vijaya Kumar[1,*], Shaik Mohammed Ibrahim[2], Giulio Lorenzini[3]

[1] Department of Mathematics, GITAM (Deemed to be University), Visakhapatnam, Andhra Pradesh 530045, India
[2] Department of Engineering Mathematics, College of Engineering, Koneru Lakshmaiah Education Foundation, Vaddeswaram, Andhra Pradesh, 522302, India
[3] Department of Engineering and Architecture, University of Parma, Parco Area delle Scienze 181/A 43124 Parma, Italy

ARTICLE INFO

Article history:
Received 17 May 2023
Received in revised form 15 July 2023
Accepted 21 July 2023
Available online 9 August 2023

Keywords:
Casson nanofluid; thermal radiation; heat source; chemical reaction; NDSolve

ABSTRACT

Casson nanofluid flow across a porous, slanted surface is investigated. In addition to the impact of a heat source, thermal energy, and a chemical reaction also are considered. Applying similarity transformations, the controlling nonlinear PDEs are converted to ODEs. To resolve the ordinary differential equations (ODEs), we used the universal numerical differential equation solver Wolfram Language function NDSolve. The distributions under heat source are affected by chemical processes and other variables are explored. While liquid velocity reduced due to inclination and the Casson factor, mass and energy transit rates rose. The findings are represented graphically and are consistent with past research. The findings would provide valuable insights into the flow patterns, temperature distribution, and concentration profiles within the system. This information can be crucial for designing and optimizing heat transfer systems, energy-efficient processes, and catalytic reactors involving Casson nanofluids and porous media.

1. Introduction

Nanofluids are a category-specific of heat transfer fluids that can be made by dispersing nanoparticles with lengths on average between 1 and 100 nm in conventional heat transfer fluids and then ensuring that the nanoparticles stay floating in the fluid. Over the past few years, scientists and engineers have discovered that even a tiny number of guest nanoparticles can significantly enhance the thermal properties of the underlying liquids.

The thermal conductivity of some nanofluids is strongly temperature and size dependent. There is a nonlinear connection between thermal conductivity, concentration and the critical heat flux at small particle concentrations of the order of 10 ppm. There are many examples of the exceptional thermal qualities of nanofluids. Due to the unique thermal transport processes, which go beyond the fundamental restrictions of the currently available macroscopic prototypes of suspensions and hence nanofluids are of enormous scientific interest. Nanofluids technology may enable the development

* *Corresponding author.*
E-mail address: vprathi@gitam.edu

https://doi.org/10.37934/arfmts.108.1.184202

of nanotechnology based coolants for a variety of innovations in the field of technology and medicine. Consequently, the study of nanofluids has become an area of scientific interest. Choi [1] was the one who initially defined nanofluids. Rusdi *et al.,* [2] studied the nanofluid penetrable flow over an exponentially shrinking sheet with thermal radiation and partial slip. The hydrodynamic and thermal behavior of a microchannel was studied by Krishna and Kumar [3] on a rectangular microchannel heat sink was done by using water, Al_2O_3-water, and TiO_2-water nanofluids as working fluids. The combined effects of viscous dissipation and Joule heating on the momentum and thermal transport for the magnetohydrodynamic flow past an inclined plate in both aiding and opposing buoyancy situations have been carried outby Das *et al.,* [4]. The study by Koriko *et al.,* [5] presents the significance of partial slip (i.e., combination of linear stretching and velocity gradient) and buoyancy on the boundary layer flow of blood-gold Carreau nanofluid over an upper horizontal surface of a paraboloid of revolution. The three nanoparticles examined by Abbas *et al.,* [6] were TiO_2, Cu, and Al_2O_3. Using water as a base and the application of differential equations, they quantitatively defined the physical state of a micropolar fluid in the presence of both weak and strong concentration. The impacts of chemical reactions as well as heat generation and absorption based on the Buongiorno model were taken into account by Rafique *et al.,* [7]. Animasaun [8] conducted research on the interactions between thermophoresis, Dufour, temperature-dependent thermal conductivity, and viscosity of an electrically conducting Casson fluid flowing down a vertical porous plate in the presence of viscous dissipation, order chemical reaction and suction. The MHD flow of Casson fluid across an exponentially stretched sheet in the midst of heat radiation has been investigated by Saidulu and Lakshmi [9].

The motion of non-Newtonian fluids is frequently employed as it has various uses. There exists a nonlinear correlation between the shear stress and the rate of shear strain when the fluid is not Newtonian. At low shear stresses, non-Newtonian fluids exhibit elastic solid behaviour that inhibits flow. Fluids that do not follow the Newtonian model include, but are not limited to, power-law fluids, micropolar fluids, viscoelastic fluids, Jeffrey fluids, Rivlin-Ericksen fluids, Casson fluids, Walter's liquid B fluids and other types of fluids. Despite the fact that a wide range of non-Newtonian fluid models have been presented to attempt to describe the behaviour of the Casson fluid but it is still considered to be one of the most significant types of non-Newtonian fluid. Synovial fluids, food processing, metallurgy, paints, coal in water, synthetic lubricants, pharmaceutical product manufacture, sewage sludge and many more substances are just some of the applications that can benefit from the usage of Casson fluid models to simulate the fluids involved in these processes. Aqueous basic plasma, which makes up the majority of human blood, is often referred to as Casson fluid since it contains numerous components such protein, fibrinogen and globin. Chain-like structures called aggregates or rouleaux are formed by human red blood cells. Reddy *et al.,* [10] conducted a numerical study of the Williamson nanofluid MHD boundary layer flow along a stretching surface with porous material while taking velocity and thermal slippage into consideration. Mukhopadhyay *et al.,* [11] used the model of Casson fluid to examine how a non-Newtonian fluid behaved in an unstable two-dimensional flow on a stretching surface with a particular surface temperature. The primary objective of Nino *et al.,* [12] was to numerically determine and experimentally compare the diameters of bubbles at various axial positions of a bioreactor being churned by a Rushton turbine. The effects of viscosity on modelling bubble dispersion in a Newtonian fluid (water) and their comparison to a non-Newtonian fluid (0.4% CMC) were particularly highlighted. Li *et al.,* [13] presented the applications of non-uniform heat source/sink and viscous dissipation in magnetohydrodynaimcs (MHD) flow of Casson nanoparticles toward a porous stretchable sheet. Hady *et al.,* [14] investigated the traits of flow as well as heat transfer of a viscoelastic nanofluid across a nonlinearly stretched sheet in the existence of thermal radiation, which is a factor in the energy equation, and variable wall

temperature. In a situation where thermal conductivity is temperature-dependent and exists in a magnetic field which is inclined, Lahmar *et al.,* [15] explored the heat transfer of an unstable nanofluid squeezed between two parallel plates. Srinivas *et al.,* [16] reviewed the hydromagnetic pulsing flow of Casson fluid in a porous channel to ascertain the temperature and chemical responses effects, and temperature-diffusion. The primary goal of Ahmadi *et al.,* [17] was to create a stable mathematical model for dusty hybrid nanofluid flow and heat transfer across a stretched sheet.

NDSolve is a robust feature of Mathematica for numerically resolving differential equations. A multitude of differential equations, including both ordinary and partial differential equations, can be solved quickly and effectively using this integrated function. The numerical methods that NDSolve chooses for seem to fit the issue structure the best automatically. The peristaltic movement of boron nitride-ethylene glycol nanofluid technology across a symmetric channel in the presence of magnetic field was thoroughly computationally analysed by Abbasi *et al.,* [18]. The energy equation incorporates thermophoresis, Brownian motion, Hall and Ohmic heating effects. NDSolve in Mathematica is applied to numerically solve the ensuing set of non-linear equations. The influences of temperature-dependent viscosity and various levels of thermal conductivity on the motion of nanoliquid in a rotating apparatus where the fluid between pairs of plates is collected were examined by Ullah *et al.,* [19]. Additionally, this investigation examines the characteristics of the modified Arrhenius energy function involving chemical reaction and the incorporation of the exponential heat source to the energy expression. Boundary layer calculations have been performed using the NDSolve technique.In their study, Anuradha and Yegammai [20] looked at the steady two-dimensional radiative MHD boundary-layer flow of a viscous, incompressible, electricity-conducting nanofluid over a vertical plate. They took into account the activation energy, viscous and ohmic dissipations, internal heat generation/absorption, and viscous and ohmic dissipations. NDsolve was used for solving of equations.

Fluid heat transport is greatly aided by its thermophysical characteristics, which may vary. The thermal conductivity and viscosity, both of which are extensively susceptible to temperature change, have an important influence on the way heat is transferred. Understanding the impact of elements such as non-linear thermal radiation, non-uniform heat sources, and the MHD flow of Williamson nanofluid across an inclined stretched sheet is essential for engineering purposes. MHD involves the study of the behavior of electrically conducting fluids in the presence of magnetic fields. It finds applications in various engineering fields, such as aerospace, nuclear engineering, and metallurgy. The interaction between magnetic fields and fluid flow can significantly affect the flow characteristics, heat transfer rates, and energy efficiency of systems. The transformation of some of the energy carried by an electric current as it passes through a resistance into heat is referred to as the joule heating process. When an electrical current flows through solid or liquid materials that transfer electricity, resistances can exist inside conductors. These resistances cause electrical energy to be converted into heat energy. The reason for this is because electrical energy can be translated into heat energy. In order to do a simulation of the consequences of MHD, a non-uniform heat source/sink, and nonlinear thermal radiation on Williamson nanofluid across an inclined stretched sheet, Srinivasulu and Bandari [21] employs the RK approach with a shooting strategy. The effect of electromagnetic force with the effect of thermal radiation on the Williamson nanofluid on a stretching surface through a porous medium was studied by Bouslimi *et al.,* [22] considering the effect of both heat generation/absorption and Joule heating. Many researchers have studied Nanofluids and its various properties [23,24].

Due to their widespread use in manufacturing, coating, polymer processing, engineering, aerodynamics, and other fields, non-Newtonian fluids have gained prominence during the past several years. Some materials that exhibit this behaviour include mud, blood, paint, and polymer

solutions. No one model can adequately capture all of the physical features of non-Newtonian fluids due to their complexity. One example of a non-Newtonian fluid with elastic solid-like properties is Casson fluid. Rafique *et al.,* [25] discussed the behaviour of micropolar nanofluid using Kelle-box method. Khan *et al.,* [26] analyses the magnetohydrodynamic flow of a double stratified micropolar fluid across a vertical stretching/ shrinking sheet in the presence of suction, chemical reaction and heat source effects. The Casson fluid model is a non-Newtonian fluid model used to describe certain types of complex fluids that exhibit yield stress behavior. The model incorporates both a viscous component as well as a yield stress component to describe the flow behavior of such fluids. One feature of the Casson fluid model is the inclusion of a yield stress term, which is the minimum stress required to initiate flow. Below this yield stress value, the fluid does not flow and behaves like a solid. When the applied stress exceeds the yield stress, the fluid starts flowing with a finite viscosity. The Casson fluid model is commonly used to describe the flow behavior of various complex fluids, such as certain types of suspensions, emulsions, and biological fluids. Its application is often seen in the food industry, pharmaceuticals, and biomedical research. Many researchers have studied Nano fluids and its various properties [27-31].

The fundamental fluid dynamics problem of fluid flow across an inclined stretched sheet has many applications in many different fields. In this case, the flow of a fluid (liquid or gas) through a solid surface that is bent at an angle and stretched or contracted in a particular direction is being studied. Fluid flow across an inclined stretching sheet is used for a variety of processes, including as thin film deposition, wire drawing, coating, and plastic extrusion. The use of inclined geometry in Casson fluid flow is motivated by various practical and scientific considerations. Some of the key motivations include understanding Casson fluid flow in inclined geometries is crucial for designing and optimizing processes in industries such as chemical engineering, petroleum engineering, geophysics, and biomedical engineering. Inclined geometries are prevalent in geophysical phenomena such as sediment transport in rivers, avalanches on inclined slopes, and flow in glaciers.

Some novel aspects have been considered. In this study, a porous nonlinear inclined plate is used to analyse the Casson nanofluid, which incorporates heat generation, thermal radiation and chemical interaction. The investigation is about how chemical reactions and other factors impact the distributions. When similarity transformations are applied to partial differential equations, the resulting equations are transformed into ordinary differential equations, which NDSolve is then able to solve. NDSolve uses a variety of numerical methods to solve ODEs and PDEs. The specific method used depends on the type of problem and the accuracy requirements. The graphical depiction includes several physical factors that have practical importance, including as energy exchange, velocity, skin friction, and concentration species. The results got are compared with results got earlier.

2. Mathematical Formulation

Casson nanofluid on an inclined, porous, nonlinear expanding plate with an angle Ω is taken into account. Here 'x' is the coordinate elevated along the stretching surface with 'a' fixed value presuming and $u_w(x) = ax^m$ and $u_\infty(x) = 0$ respectively, stand for the stretching and free stream speeds, respectively. Brownian motion's characteristics are taken into consideration. Discussions also touch on temperature source, chemical responses, suction, and injection. In linear radiative heat transfer, the heat flux is directly proportional to the temperature gradient, and the relationship can be described by a linear equation. This implies that the heat transfer rate remains proportional to the temperature difference between the hot and cold regions. Linear radiative heat transfer is

applicable when temperature differences are small, and the medium through which the heat is transferred behaves in a linear manner.

The rheological equation of state for an isotropic and incompressible flow of Casson fluid is

$$\tau_{ij} = \begin{cases} 2\left(\mu_B + \dfrac{p_y}{\sqrt{2\pi}}\right)e_{ij}, & \pi > \pi_c \\ 2\left(\mu_B + \dfrac{p_y}{\sqrt{2\pi_c}}\right)e_{ij}, & \pi_c > \pi \end{cases}$$

where μ_B is the plastic dynamic viscosity of the non-Newtonian fluid, p_y is the yield stress of the fluid, π is the product of the component of deformation rate with itself, $\pi = e_{ij}e_{ij}$, e_{ij} is the $(i,j)^{th}$ component of the deformation rate and π_c is the critical value of this product based on the non-Newtonian model.

Figure 1 depicts the physical prototype and the coordinate system. Following are the boundary layer equations given the above mentioned restrictions [7].

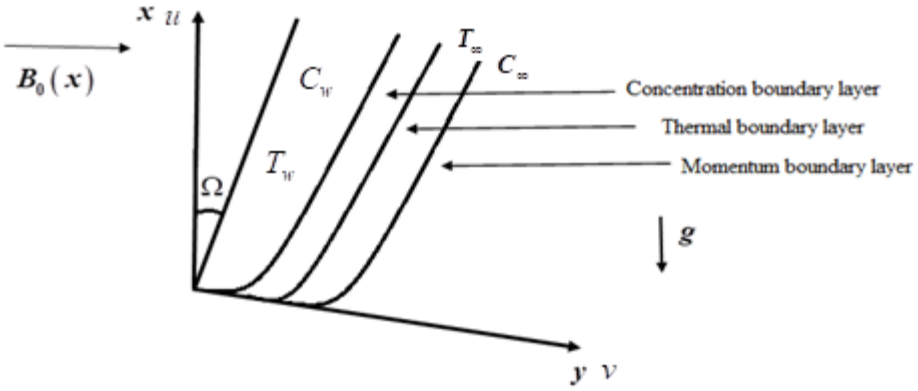

Fig. 1. Physical geometry and coordinate system

The flow equations are as follows

$$\frac{\partial u}{\partial x} + \frac{\partial v}{\partial y} = 0, \tag{1}$$

$$u\frac{\partial u}{\partial x} + v\frac{\partial u}{\partial y} = v\left(1+\frac{1}{\beta}\right)\frac{\partial^2 u}{\partial y^2} + g[\beta_t(T-T_\infty) + \beta_c(C-C_\infty)]\cos\Omega - \left(\frac{\sigma B^2{}_0}{\rho_f}\right)u, \tag{2}$$

$$u\frac{\partial T}{\partial x} + v\frac{\partial T}{\partial y} = \alpha\frac{\partial^2 T}{\partial y^2} + \tau\left[D_B\frac{\partial C}{\partial y}\frac{\partial T}{\partial y} + \frac{D_T}{T_\infty}\left(\frac{\partial T}{\partial y}\right)^2\right] + \frac{Q_0}{(\rho C)_f}(T-T_\infty) - \frac{1}{(\rho C)_f}\frac{\partial q_r}{\partial y}, \tag{3}$$

$$u\frac{\partial C}{\partial x} + v\frac{\partial C}{\partial y} = D_B\frac{\partial^2 C}{\partial y^2} + \frac{D_T}{T_\infty}\frac{\partial^2 T}{\partial y^2} - K^*(C-C_\infty) \tag{4}$$

Velocity components in x, y directions are u, v respectively, g is the gravity related acceleration, B_0 is the uniform magnetic field strength , σ is the electrical conductivity, β_t is factor of Thermal extension, β_c represents factor of concentration enlargement, q_r is radiative heat flux, D_B is Brownian diffusion factor and D_T is thermophoresis diffusion factor, Q_0 is the absorption or heat generation coefficient, κ^* is the chemical reaction $\tau = \frac{(\rho C)_f}{(\rho C)_p}$ is fraction of heat capability of nanofluid to the base fluid, $(\rho C)_p$ is the heat capacity of nanoparticles, $(\rho C)_f$ is the heat capacity of the liquid, $\alpha = \frac{k}{(\rho C)_f}$ is the thermal diffusivity, K^* is the dimensional chemical reaction.

The subjected boundary conditions are

$$u = u_w(x) = ax^m, v = V_w, T = T_w, C = C_w \text{ at } y = 0,$$
$$u \to 0, v \to 0, T \to T_\infty, C \to C_\infty \text{ as } y \to \infty. \quad (5)$$

Following Rosseland approximation, the radiative heat flux is

$$q_r = -\frac{4\sigma^* \partial T^4}{3k^* \partial y}$$

where Stefan Boltzman constant is σ^* and k^* is the mean absorption coefficient. Additionally, we presume that the flow's internal temperature differential is adequately large so that T^4 is represented as a linear function of temperature. As a result, by expanding T^4 in Taylor series about T_∞ If we ignore terms of higher order, we get

$$T^4 \cong 4T_\infty{}^3 T - 3T_\infty{}^4$$

Here the nonlinear ordinary differential equations obtained by using stream function $\psi = \psi(x, y)$

$$u = \frac{\partial \psi}{\partial y}, v = -\frac{\partial \psi}{\partial x} \quad (6)$$

where Eq. (1) is fulfilled identically. The similarity transformations are

$$\psi = \sqrt{\frac{2vax^{m-1}}{m+1}} f(\eta), \eta = y\sqrt{\frac{(m+1)ax^m}{2v}}, \theta(\eta) = \frac{T - T_\infty}{T_w - T_\infty}, \phi(\eta) = \frac{C - C_\infty}{C_w - C_\infty}. \quad (7)$$

On substitution of Eq. (7) in Eq. (2) to Eq. (4) reduces to the following nonlinear ordinary differential equations

$$\left(1 + \frac{1}{\beta}\right) f''' + ff'' - \left(\frac{2m}{m+1}\right) f'^2 + \frac{2}{m+1}(Gr_x\theta + Gc_x\phi)\cos\Omega - \left(\frac{2M}{m+1}\right) f' = 0, \quad (8)$$

$$\frac{1}{\Pr}\left(1+\frac{4R}{3}\right)\theta''+f\theta'+Q\theta+Nb\phi'\theta'+Nt\theta'^{2}=0, \tag{9}$$

$$\phi''+Le^{*}\Pr f\phi'+Nt_{b}\theta''-Le^{*}\Pr C_{r}\phi=0. \tag{10}$$

where $M=\left(\frac{\sigma B^{2}{}_{0}}{a\rho}\right)$ is magnetic parameter, $Le=\frac{\nu}{D_B}$ is the Lewis number, $\Pr=\frac{\nu}{\alpha}$ is the Prandtl number, $Nb=\frac{\tau D_B\left(C_w-C_\infty\right)}{\nu}$ is the Brownian motion parameter, $Nt=\frac{\tau D_t\left(T_w-T_\infty\right)}{\nu T_\infty}$ is the thermophoresis parameter, $Gr_x=\frac{g\beta_t\left(T_w-T_\infty\right)x^{-2m+1}}{a^2}$, $Nt_b=\frac{N_t}{N_b}$, $Q=\frac{Q_0}{a\left(\rho C\right)_f}$ is the heat generation/absorption parameter, $Gc_x=\frac{g\beta_c\left(C_w-C_\infty\right)x^{-2m+1}}{a^2}$, $C_r=\frac{K^{*}}{a}$ is the chemical reaction parameter, $R=\frac{16\sigma^{*}T_\infty^{3}}{3kk^{*}}$ is radiation parameter, $\mathrm{Re}_x=\frac{u_w\left(x\right)x}{\nu}$ is the local Reynolds number (11)

Here Gr_x signifies the local Local Grashof number, Gc_x denotes the local modified Local Grashof number, in order to eliminate x from local Local Grashof number and local modified Local Grashof number , the coefficient of thermal expansion β_t and coefficient of concentration expansion β_c are proportional to x^1 .We assume that [25,26]

$$\beta_t=nx^{2m-1},\beta_c=n_1x^{2m-1} \tag{12}$$

As n, n_1 have fixed values, and so Gr_x, Gc_x are $Gr=\frac{gn\left(T_w-T_\infty\right)}{a^2},Gc=\frac{gn_1\left(C_w-C_\infty\right)}{a^2}$ are the local Grashof and local modified Local Grashof number.

The boundary settings undergo modifications to

$$f\left(\eta\right)=S,f'\left(\eta\right)=1,\theta\left(\eta\right)=1,\phi\left(\eta\right)=1 \text{ at } \eta=0,$$
$$f'\left(\eta\right)\to 0,\theta\left(\eta\right)\to 0,\phi\left(\eta\right)\to 0 \text{ as } \eta\to 0 . \tag{13}$$

Where $S=$ is the suction/injection parameter.

The skin friction, Sherwood number, and Nusselt number for the current study are

$$Nu_x=\frac{xq_w}{k\left(T_w-T_\infty\right)},Sh_x=\frac{xq_m}{D_B\left(C_w-C_\infty\right)},C_f=\frac{\tau_w}{\frac{1}{2}u^{2}{}_{w}\rho_f} \tag{14}$$

where $\tau_w = \mu\left(1+\frac{1}{\beta}\right)\frac{\partial u}{\partial y}$, $q_w = -\left(k+\frac{16\sigma^* T^3{}_\infty}{3k^*}\right)\frac{\partial T}{\partial y}$, $q = -D_B\frac{\partial C}{\partial y}$ at $y=0$

$\mathrm{Re}_x = \frac{u_w(x)\,x}{\nu}$ is the local Reynolds number

$$\therefore C_{fx}(0) = \left(1+\frac{1}{\beta}\right) f''(0) = \frac{C_f}{2}\sqrt{\frac{2}{m+1}\mathrm{Re}_x},$$

$$-\left(1+\frac{4R}{3}\right)\theta'(0) = \frac{Nu_x}{\sqrt{\frac{m+1}{2}\mathrm{Re}_x}},$$

$$-\phi'(0) = \frac{Sh_x}{\sqrt{\frac{m+1}{2}\mathrm{Re}_x}}$$

3. Results and Discussion

The numerical outcomes of the converted nonlinear ordinary differential Eq. (8) to Eq. (10) along with Eq. (13) are deduced by NDSolve in Mathematica. Tables and figures are arranged for the quantities and parameters of our concern Nb (Brownian motion parameter), Nt (thermophoresis parameter), C_r (Chemical reaction constraint), M (magnetic factor), Gr (local Local Grashof number), Q (heat generation or absorption bound), Gc (local modified Local Grashof number), Ω (inclination parameter), β (Casson fluid parameter), Pr (Prandtl number), Le (Lewis number), S (suction or injection parameter), R (Radiation parameter). Some of the figures are generated by varying the value of a parameter within a predetermined range, while others, are always maintained at the same value such as

$$\beta = 1.0, m = 0.5, Gr = R = M = Q = S = Nb = Nt = 0.1, Gc = 0.9,\ \mathrm{Pr} = 6.5, Le = 5.0, C_r = 0.5,$$
$$\Omega = \pi/4.$$

Table 1 presents the results of reduced Nusselt number $-\theta'(0)$ and reduced Sherwod number $-\phi'(0)$ compared with existing outcomes of Khan and Pop [32] with $M = S = R = Gr = Gc = C_r = Q = 0, \mathrm{Pr} = Le = 10, m = 1$ and $\Omega = 90^0$ when $\beta \to \infty$.

Table 1
Contrast of the reduced Nusselt number $-\theta'(0)$ and reduced Sherwod number $-\phi'(0)$ with $M = S = R = Gr = Gc = C_r = Q = 0, \mathrm{Pr} = Le = 10, m = 1$ and $\Omega = 90^0$ when $\beta \to \infty$

Nb	Nt	Khan and Pop [32]		Rafique *et al.,* [7]		Current outcomes	
		$-\theta'(0)$	$-\phi'(0)$	$-\theta'(0)$	$-\phi'(0)$	$-\theta'(0)$	$-\phi'(0)$
0.1	0.1	0.9524	2.1294	0.9524	2.1294	0.952380	2.129406
0.2	0.2	0.3654	2.5152	0.3654	2.5152	0.365359	2.515236
0.3	0.3	0.1355	2.6088	0.1355	2.6088	0.135514	2.608832
0.4	0.4	0.0495	2.6038	0.0495	2.6038	0.049465	2.603858

In the investigation of fluid's properties, velocity distributions are crucial. The magnetic field has a considerable impact on the movement of fluids. The velocity outline plunges as the magnetic field limitation M is on the rise, as shown in Figure 2. The Lorentz force, which is produced by a magnetic field and slows down a liquid's velocity, provides the basis for this theory. Additionally, Jafar's *et al.,* [33] velocity profile analysis yielded comparable results.

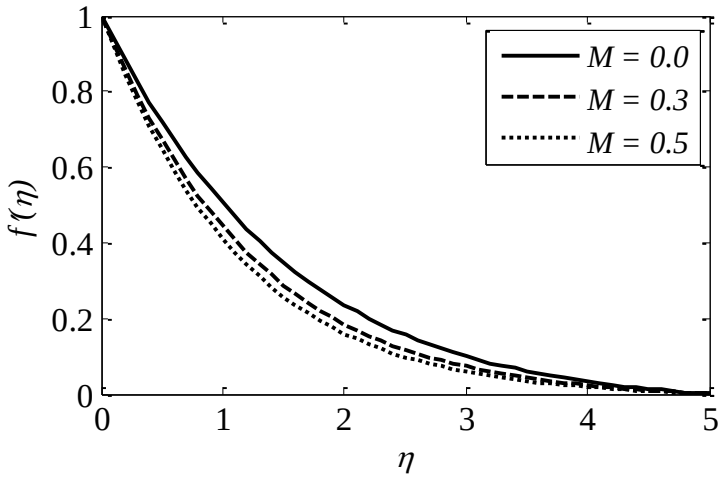

Fig. 2. Effect of M on velocity profile

Figure 3 displays the slowed velocity profile for large quantity of the non-linear stretching parameter m. When m gets higher, the material properties of the framework induce the thickness of the momentum boundary layer to shrink.

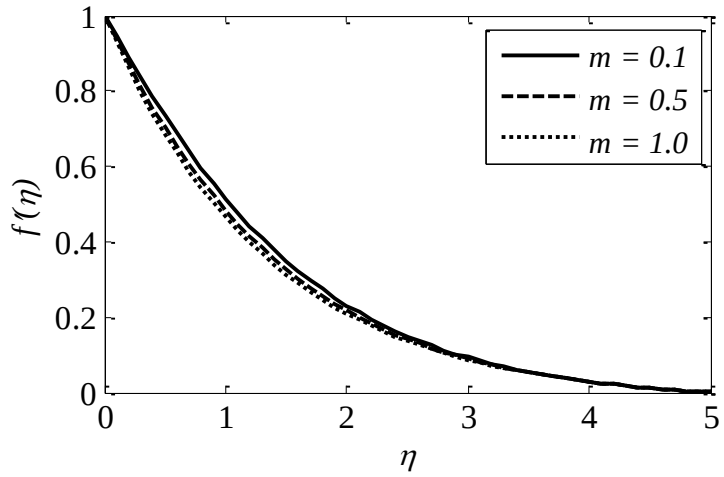

Fig. 3. Effect of m on velocity profile

The consequence of the inclination parameter Ω on the velocity outline is clarified and shown in Figure 4. Looking at figure demonstrates that the velocity contour decreases as the values of Ω increase. The circumstances also suggest that the gravitational force acting on flow will be at its strongest when $\Omega = 0^0$. This is because the sheet will be vertical at this moment. But if $\Omega = 90^0$, the sheet will be horizontal, because of which there will be decline in the velocity profile due to the decreased strength of the bouncing forces.

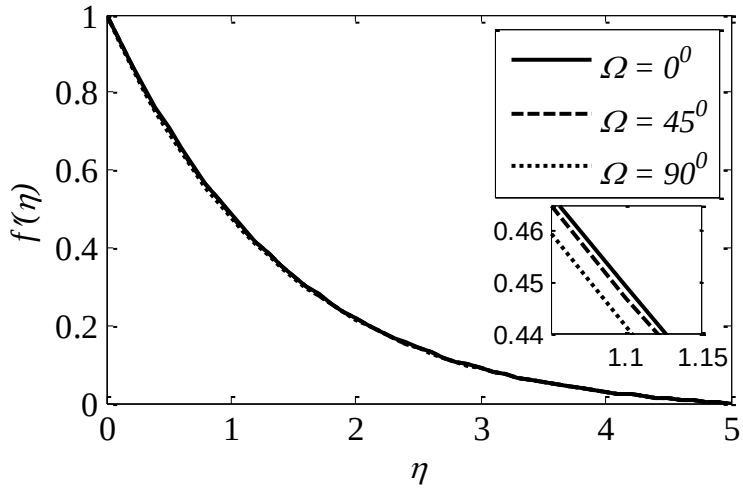

Fig. 4. Effect of Ω on velocity profile

The influence of β the Casson constraint on velocity factor is depicted in Figure 5. It is detected that for various values of β velocity profile diminishes. The cause overdue this behaviour is that by enhancing the values of β the fluid viscosity enhances, i.e., sliding down the yield stress. Which leads to a reduction in momentum boundary layer thickness. Therefore, the momentum boundary layer thickness reduces.

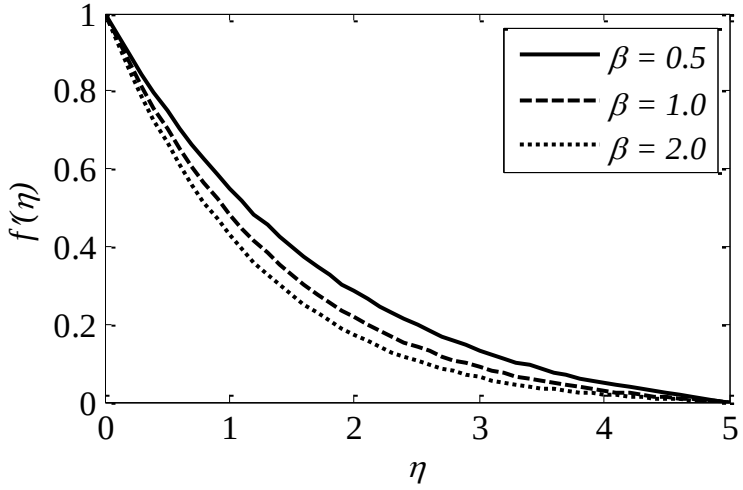

Fig. 5. Effect of β on velocity profile

The effects of suction parameter S on the velocity profile are shown in Figure 6. As S parameter increases, the velocity trend appears to be dropping, indicating the common fact that suction maintains the boundary layer's growth and consequently reduces the formation of the highest points in the velocity outline.

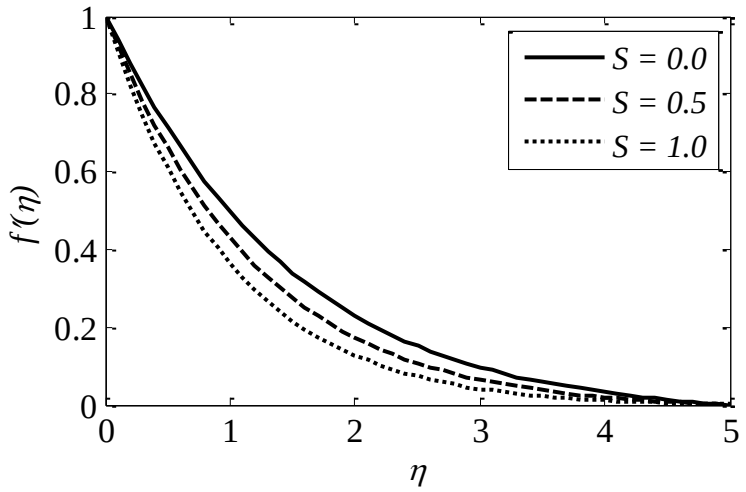

Fig. 6. Effect of S on velocity profile

Figure 7 illustrates the impact thermal local Grashof number Gr has on the velocity. When is Gr raised, the velocity also improves. This is because buoyancy, which affects particles of fluid as a result of gravitational force, and in turn boosts the fluid's velocity.

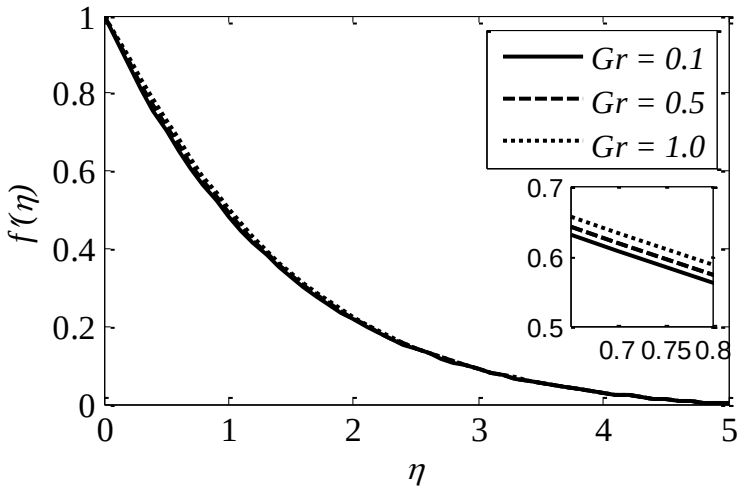

Fig. 7. Effect of Gr on velocity profile

Expanding the solutal buoyancy factor Gc, which is apparent in Figure 8, improves the velocity profile. The buoyancy parameter, in a physical sense, lowers the viscous forces that trigger the velocity to go up.

The main difference between the local Grashof number and the modified local Grashof number lies in their definitions. The local Grashof number considers the ratio of buoyancy forces to viscous forces alone and is typically used in natural convection problems, where buoyancy is the dominant driving force. On the other hand, the modified Local Grashof number includes an additional characteristic velocity scale, making it suitable for situations where buoyancy forces are not the sole driving force, and external forces play a significant role in the fluid flow. It's important to note that the choice between the local Grashof number and the modified local Grashof number depends on the specific problem at hand and the dominant driving forces in the flow. Each parameter has its significance and applications in different scenarios, and both can provide valuable insights into fluid flow and heat transfer phenomena.

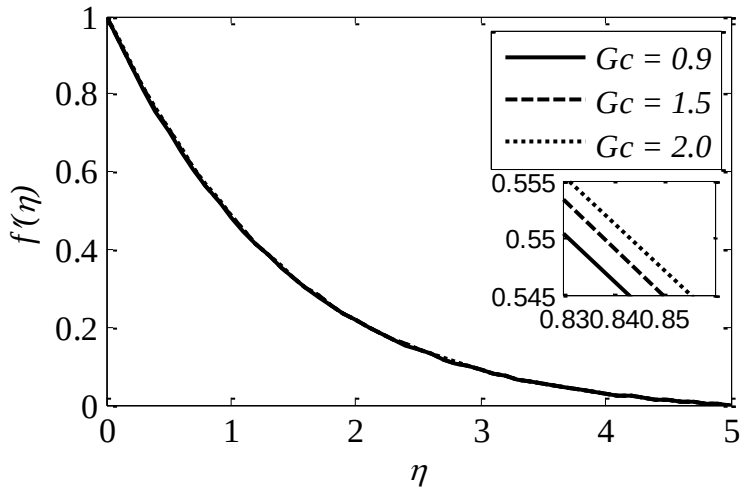

Fig. 8. Effect of Gc on velocity profile

Figure 9 demonstrates that when the radiation parameter R expands, so does the temperature. Increases in surface heat flow caused by increasing radiation input led to a steeper raise in fluid temperature.

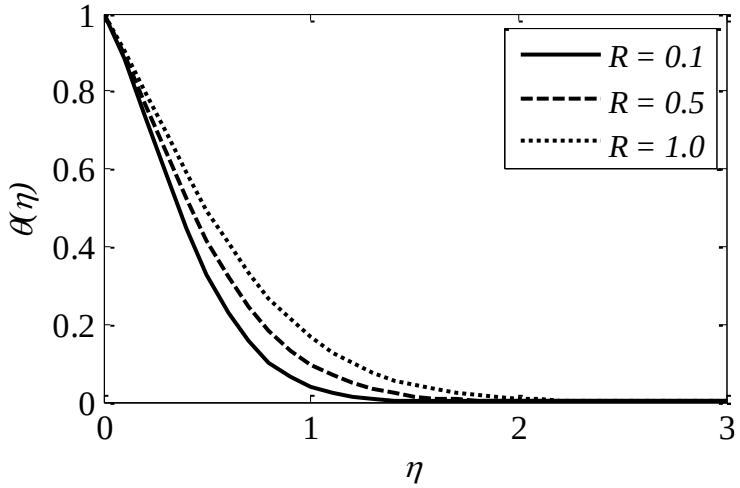

Fig. 9. Effect of R on Temperature profile

Figure 10 highlights that as the values of the heat generation Q constraint get higher, the temperature curves expand. The thermal boundary layer's temperature rises with the levels of ascent, increasing the liquid's velocity and allowing heat to accumulate in the flow region.

The implications of the Prandtl number (Pr) on the temperature and concentration profile is outlined in Figure 11 and Figure 12 for a variety of Pr values. When working with bigger amounts of Pr, ought to have less thermal diffusion. As a result, temperature and concentration profiles flatten out as the Pr value rise.

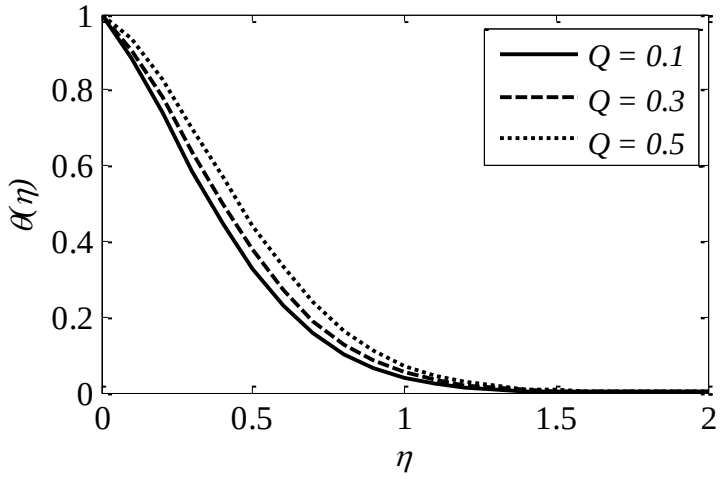

Fig. 10. Effect of Q on Temperature profile

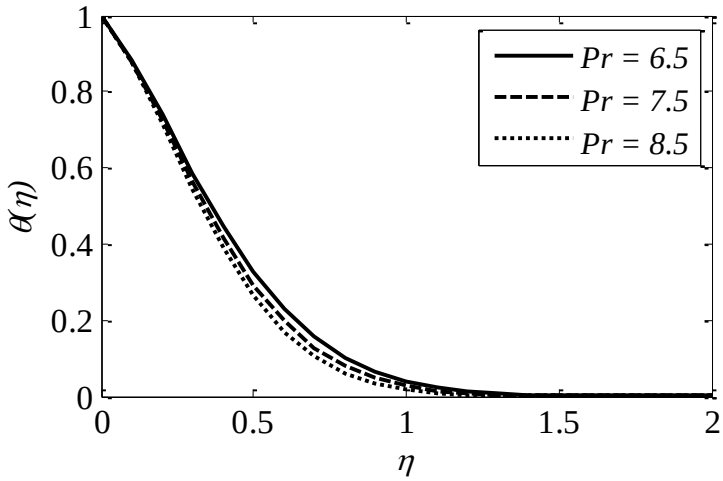

Fig. 11. Effect of $\Pr$ on Temperature profile

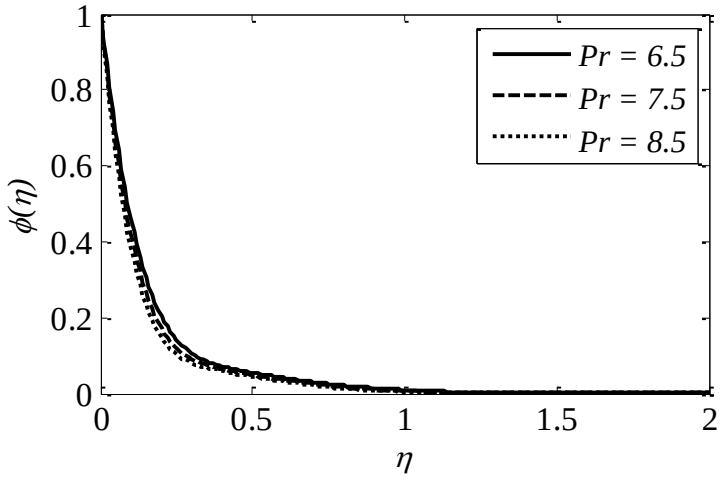

Fig. 12. Effect of $\Pr$ on Concentration profile

Brownian motion's (Nb) impact on the temperature as well as concentration profiles is potrayed in Figure 13 and Figure 14. The temperature sketch climbs as Nb increases, but the concentration distribution reveals a distinct pattern. The physical reason for the boundary layer heating up is the

emerging Brownian motion, which is anticipated to transport nanoparticles from the expanding sheet to the stagnant liquid. There are therefore fewer nanoparticles to absorb as a result.

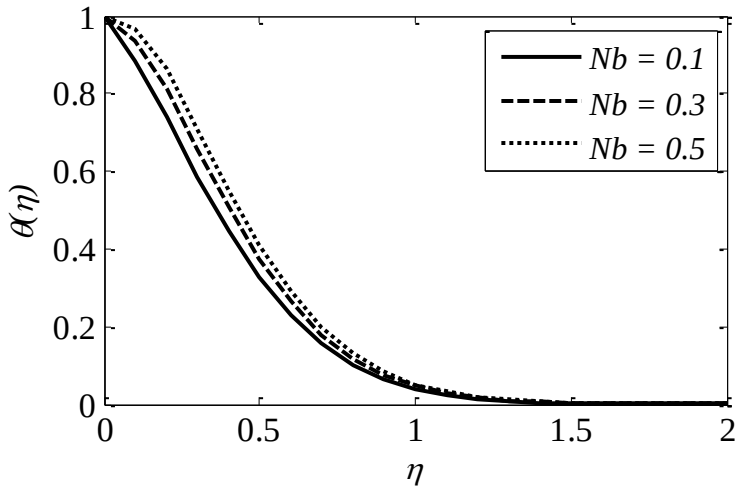

Fig. 13. Effect of Nb on Temperature profile

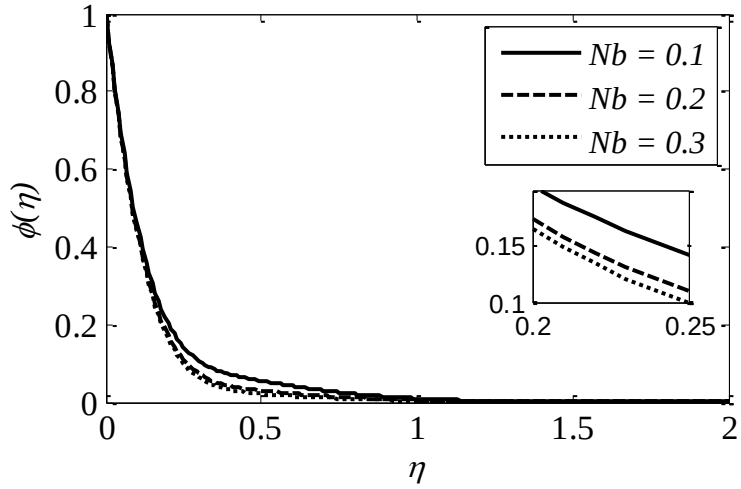

Fig. 14. Effect of Nb on Concentration profile

The implications of the thermophoresis parameter Nt on the concentration as well as temperature profile is apparent in Figure 15 and Figure 16. When Nt becomes higher, nanoparticles shift from warmer to cooler regions as their concentration and temperature elevate due to a stronger thermophoretic force.

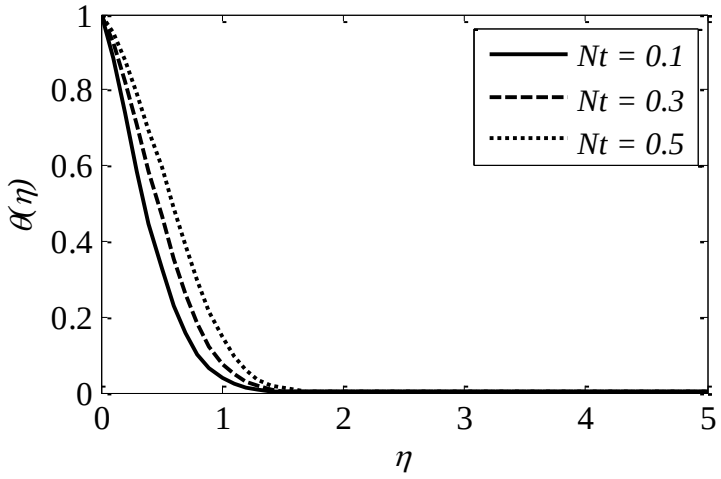

Fig. 15. Effect of Nt on Temperature profile

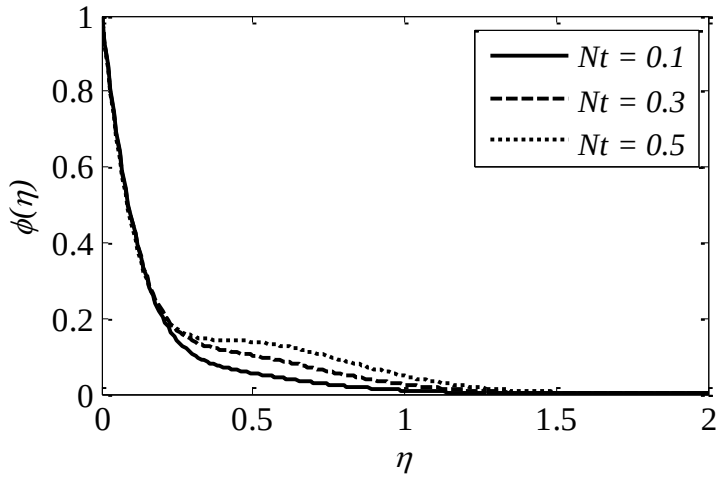

Fig. 16. Effect of Nt on Concentration profile

The ratio of heat diffusivity to mass diffusivity is known as the Lewis number. When heat and mass are being transferred simultaneously through fluid fluxes, the Lewis number is employed to describe the flow. Lifting the value of Lewis number Le induces a surge in the thermal boundary layer thickness, but it additionally culminates in a drop in the thickness of the concentration boundary layer. This is shown in Figure 17.

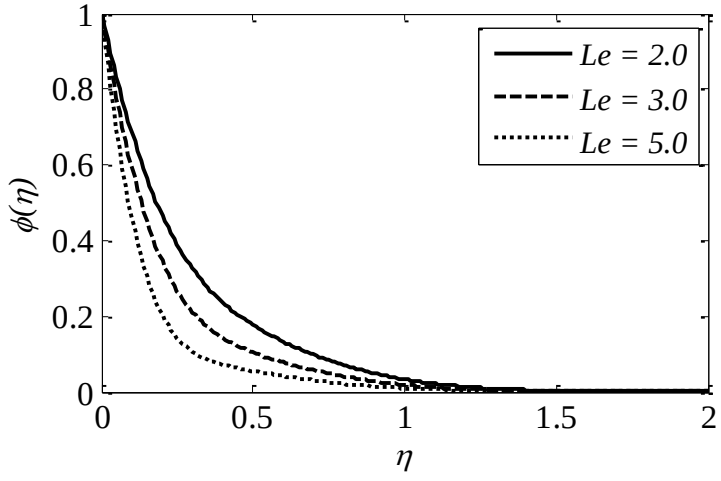

Fig. 17. Effect of Le on Concentration profile

Figure 18 depicts how a chemical reaction parameter affects concentration profiles. It is known that the concentration drops as the chemical reaction parameter grows.

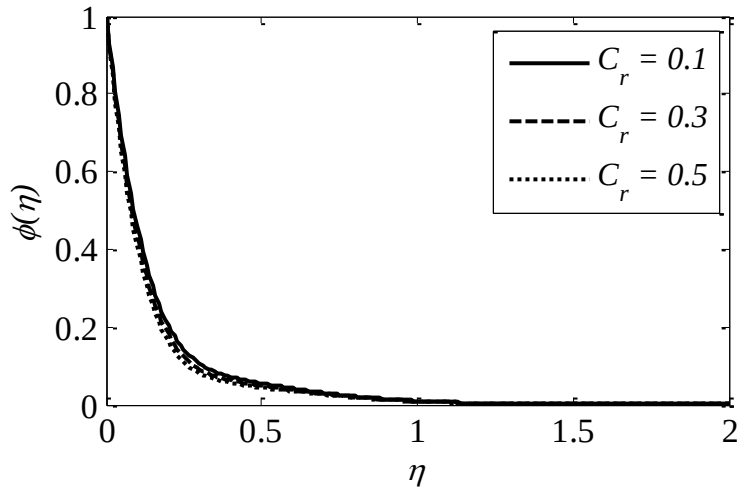

Fig. 18. Effect of C_r on Concentration profile

From Figure 19 to Figure 21, it is clear that $-\theta'(0)$ and $-\phi'(0)$ diminish with parameters Ω and M but these parameters have opposite influence on $C_{fx}(0)$.

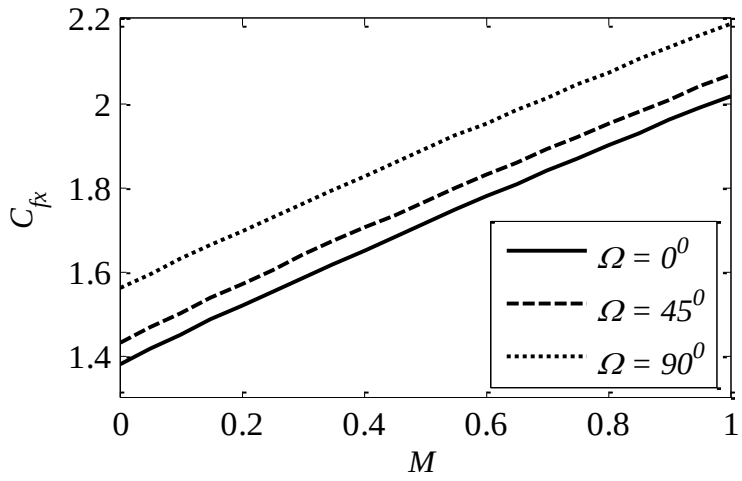

Fig. 19. Effect of Ω and M on C_{fx}

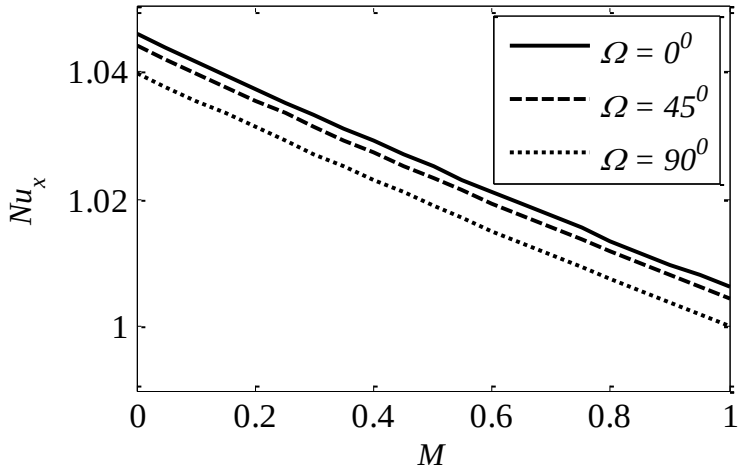

Fig. 20. Effect of Ω and M on Nu_x

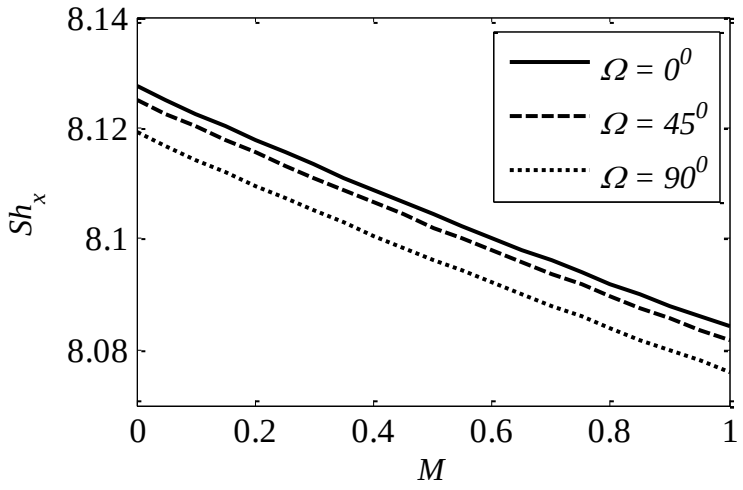

Fig. 21. Effect of Ω and M on Sh_x

4. Conclusion

The energy and species transfer in nonlinear slanted stretching sheets of the Casson type nanofluid flow were examined. The effects of a heat source, suction or injection, radiation, and chemical reaction on the rates of mass and energy transfer are studied numerically. The following are crucial points for the conclusion.

i. Fluid velocity decreases as the inclination factor increases.
ii. The local Local Grashof number and the local modified Local Grashof number increase, which improves the velocity profile.
iii. Radiation enhances the temperature.
iv. The rates of energy as well as mass transport diminish by rising inclination.
v. The fluid's velocity drops with the Casson parameter.
vi. Concentration profile grows as a result of chemical reaction factor rise.
vii. An increase of the inclination parameter enhances the skin friction coefficient but has the reverse impact on reduced Sherwood as well as Nusselt numbers.

The results obtained in this study will be used to analyse the heat and mass transport features in many non-newtonian nanofluid flow industrial applications. This work can be extended in future with some other geometries and physical conditions.

Acknowledgement
We appreciate the reviewer's spending time and making the effort to read the manuscript. We sincerely thank you for your insightful comments and recommendations, which allowed us to increase the manuscript's quality.

References

[1] Choi, Stephen US. "Nanofluids: from vision to reality through research." *ASME Journal of Heat and Mass Transfer* 131, no. 3 (2009): 033106. https://doi.org/10.1115/1.3056479
[2] Rusdi, Nadia Diana Mohd, Siti Suzilliana Putri Mohamed Isa, Norihan Md Arifin, and Norfifah Bachok. "Thermal Radiation in Nanofluid Penetrable Flow Bounded with Partial Slip Condition." *CFD Letters* 13, no. 8 (2021): 32-44. https://doi.org/10.37934/cfdl.13.8.3244
[3] Krishna, V. Murali, and M. Sandeep Kumar. "Numerical analysis of forced convective heat transfer of nanofluids in microchannel for cooling electronic equipment." *Materials Today: Proceedings* 17 (2019): 295-302. https://doi.org/10.1016/j.matpr.2019.06.433
[4] Das, S., R. N. Jana, and O. D. Makinde. "Magnetohydrodynamic mixed convective slip flow over an inclined porous plate with viscous dissipation and Joule heating." *Alexandria Engineering Journal* 54, no. 2 (2015): 251-261. https://doi.org/10.1016/j.aej.2015.03.003
[5] Koriko, Olubode K., I. L. Animasaun, B. Mahanthesh, S. Saleem, G. Sarojamma, and R. Sivaraj. "Heat transfer in the flow of blood-gold Carreau nanofluid induced by partial slip and buoyancy." *Heat Transfer-Asian Research* 47, no. 6 (2018): 806-823. https://doi.org/10.1002/htj.21342
[6] Abbas, Nadeem, S. Saleem, S. Nadeem, A. A. Alderremy, and A. U. Khan. "On stagnation point flow of a micro polar nanofluid past a circular cylinder with velocity and thermal slip." *Results in Physics* 9 (2018): 1224-1232. https://doi.org/10.1016/j.rinp.2018.04.017
[7] Rafique, K., M. A. Imran, M. I. Anwar, M. Misiran, and A. Ahmadian. "Energy and mass transport of Casson nanofluid flow over a slanted permeable inclined surface." *Journal of Thermal Analysis and Calorimetry* 144 (2021): 2031-2042. https://doi.org/10.1007/s10973-020-10481-9
[8] Animasaun, I. L. "Effects of thermophoresis, variable viscosity and thermal conductivity on free convective heat and mass transfer of non-darcian MHD dissipative Casson fluid flow with suction and nth order of chemical reaction." *Journal of the Nigerian Mathematical Society* 34, no. 1 (2015): 11-31.
[9] Saidulu, N., and A. Venkata Lakshmi. "Slip effects on MHD flow of Casson fluid over an exponentially stretching sheet in presence of thermal radiation, heat source/sink and chemical reaction." *European Journal of Advances in Engineering and Technology* 3, no. 1 (2016): 47-55.
[10] Reddy, Y. Dharmendar, Fateh Mebarek-Oudina, B. Shankar Goud, and A. I. Ismail. "Radiation, velocity and thermal slips effect toward MHD boundary layer flow through heat and mass transport of Williamson nanofluid with porous medium." *Arabian Journal for Science and Engineering* 47, no. 12 (2022): 16355-16369. https://doi.org/10.1007/s13369-022-06825-2
[11] Mukhopadhyay, Swati, Prativa Ranjan De, Krishnendu Bhattacharyya, and G. C. Layek. "Casson fluid flow over an unsteady stretching surface." *Ain Shams Engineering Journal* 4, no. 4 (2013): 933-938. https://doi.org/10.1016/j.asej.2013.04.004
[12] Nino, Lilibeth, Ricardo Gelves, Haider Ali, Jannike Solsvik, and Hugo Jakobsen. "Numerical determination of bubble size distribution in Newtonian and non-Newtonian fluid flows based on the complete turbulence spectrum." *Chemical Engineering Science* 253 (2022): 117543. https://doi.org/10.1016/j.ces.2022.117543
[13] Li, Yun-Xiang, M. Israr Ur Rehman, Wen-Hua Huang, M. Ijaz Khan, Sami Ullah Khan, Ronnason Chinram, and S. Kadry. "Dynamics of Casson nanoparticles with non-uniform heat source/sink: A numerical analysis." *Ain Shams Engineering Journal* 13, no. 1 (2022): 101496. https://doi.org/10.1016/j.asej.2021.05.010
[14] Hady, Fekry M., Fouad S. Ibrahim, Sahar M. Abdel-Gaied, and Mohamed R. Eid. "Radiation effect on viscous flow of a nanofluid and heat transfer over a nonlinearly stretching sheet." *Nanoscale Research Letters* 7 (2012): 1-13. https://doi.org/10.1186/1556-276X-7-229
[15] Lahmar, Sihem, Mohamed Kezzar, Mohamed R. Eid, and Mohamed Rafik Sari. "Heat transfer of squeezing unsteady nanofluid flow under the effects of an inclined magnetic field and variable thermal conductivity." *Physica A: Statistical Mechanics and Its Applications* 540 (2020): 123138. https://doi.org/10.1016/j.physa.2019.123138

[16] Srinivas, Suripeddi, Challa Kalyan Kumar, and Anala Subramanyam Reddy. "Pulsating flow of Casson fluid in a porous channel with thermal radiation, chemical reaction and applied magnetic field." *Nonlinear Analysis: Modelling and Control* 23, no. 2 (2018): 213-233. https://doi.org/10.15388/NA.2018.2.5

[17] Ahmadi, Mohammad Hossein, Amin Mirlohi, Mohammad Alhuyi Nazari, and Roghayeh Ghasempour. "A review of thermal conductivity of various nanofluids." *Journal of Molecular Liquids* 265 (2018): 181-188. https://doi.org/10.1016/j.molliq.2018.05.124

[18] Abbasi, F. M., Maimoona Gul, and S. A. Shehzad. "Hall effects on peristalsis of boron nitride-ethylene glycol nanofluid with temperature dependent thermal conductivity." *Physica E: Low-Dimensional Systems and Nanostructures* 99 (2018): 275-284. https://doi.org/10.1016/j.physe.2018.02.006

[19] Ullah, Ikram, Metib Alghamdi, Wei-Feng Xia, Syed Irfan Shah, and Hamid Khan. "Activation energy effect on the magnetized-nanofluid flow in a rotating system considering the exponential heat source." *International Communications in Heat and Mass Transfer* 128 (2021): 105578. https://doi.org/10.1016/j.icheatmasstransfer.2021.105578

[20] Anuradha, S., and M. Yegammai. "MHD radiative boundary layer flow of nanofluid past a vertical plate with effects of binary chemical reaction and activation energy." *Global Journal of Pure and Applied Mathematics* 13, no. 9 (2017): 6377-6392.

[21] Srinivasulu, T., and Shankar Bandari. "MHD, Nonlinear thermal radiation and non-uniform heat source/sink effect on Williamson nanofluid over an inclined stretching sheet." *Malaya J. Matematik (MJM)* 8, no. 3 (2020): 1337-1345. https://doi.org/10.26637/MJM0803/0106

[22] Bouslimi, Jamal, M. Omri, R. A. Mohamed, K. H. Mahmoud, S. M. Abo-Dahab, and M. S. Soliman. "MHD Williamson nanofluid flow over a stretching sheet through a porous medium under effects of joule heating, nonlinear thermal radiation, heat generation/absorption, and chemical reaction." *Advances in Mathematical Physics* 2021 (2021). https://doi.org/10.1155/2021/9950993

[23] Reddy, Yanala Dharmendar, Dodda Ramya, and Laxmianarayanagari Anand Babu. "Effect of thermal radiation on MHD boundary layer flow of nanofluid and heat transfer over a non-linearly stretching sheet with transpiration." *Journal of Nanofluids* 5, no. 6 (2016): 889-897. https://doi.org/10.1166/jon.2016.1284

[24] Bing, Kho Yap, Abid Hussanan, Muhammad Khairul Anuar Mohamed, Norhafizah Mohd Sarif, Zulkhibri Ismail, and Mohd Zuki Salleh. "Thermal radiation effect on MHD flow and heat transfer of Williamson nanofluids over a stretching sheet with Newtonian heating." In *AIP Conference Proceedings*, vol. 1830, no. 1. AIP Publishing, 2017. https://doi.org/10.1063/1.4980885

[25] Rafique, Khuram, Muhammad Imran Anwar, Masnita Misiran, Ilyas Khan, Asiful H. Seikh, El-Sayed M. Sherif, and Kottakkaran Sooppy Nisar. "Keller-box simulation for the buongiorno mathematical model of micropolar nanofluid flow over a nonlinear inclined surface." *Processes* 7, no. 12 (2019): 926. https://doi.org/10.3390/pr7120926

[26] Khan, Ansab Azam, Khairy Zaimi, Suliadi Firdaus Sufahani, and Mohammad Ferdows. "MHD flow and heat transfer of double stratified micropolar fluid over a vertical permeable shrinking/stretching sheet with chemical reaction and heat source." *Journal of Advanced Research in Applied Sciences and Engineering Technology* 21, no. 1 (2020): 1-14. https://doi.org/10.37934/araset.21.1.114

[27] Abbasi, A., Sami Ullah Khan, Kamel Al-Khaled, M. Ijaz Khan, W. Farooq, Ahmed M. Galal, Khurram Javid, and M. Y. Malik. "Thermal prospective of Casson nano-materials in radiative binary reactive flow near oblique stagnation point flow with activation energy applications." *Chemical Physics Letters* 786 (2022): 139172. https://doi.org/10.1016/j.cplett.2021.139172

[28] Teh, Yuan Ying, and Adnan Ashgar. "Three dimensional MHD hybrid nanofluid Flow with rotating stretching/shrinking sheet and Joule heating." *CFD Letters* 13, no. 8 (2021): 1-19. https://doi.org/10.37934/cfdl.13.8.119

[29] Raza, Ali, Sami Ullah Khan, Kamel Al-Khaled, M. Ijaz Khan, Absar Ul Haq, Fakhirah Alotaibi, A. Mousa Abd Allah, and Sumaira Qayyum. "A fractional model for the kerosene oil and water-based Casson nanofluid with inclined magnetic force." *Chemical Physics Letters* 787 (2022): 139277. https://doi.org/10.1016/j.cplett.2021.139277

[30] Al-Khaled, Kamel, and Sami Ullah Khan. "Thermal aspects of casson nanoliquid with gyrotactic microorganisms, temperature-dependent viscosity, and variable thermal conductivity: Bio-technology and thermal applications." *Inventions* 5, no. 3 (2020): 39. https://doi.org/10.3390/inventions5030039

[31] Kumar, Bharath, and Suripeddi Srinivas. "Unsteady hydromagnetic flow of Eyring-Powell nanofluid over an inclined permeable stretching sheet with joule heating and thermal radiation." *Journal of Applied and Computational Mechanics* 6, no. 2 (2020): 259-270.

[32] Khan, W. A., and I. Pop. "Boundary-layer flow of a nanofluid past a stretching sheet." *International Journal of Heat and Mass Transfer* 53, no. 11-12 (2010): 2477-2483. https://doi.org/10.1016/j.ijheatmasstransfer.2010.01.032

[33] Jafar, Ahmad Banji, Sharidan Shafie, and Imran Ullah. "MHD radiative nanofluid flow induced by a nonlinear stretching sheet in a porous medium." *Heliyon* 6, no. 6 (2020). https://doi.org/10.1016/j.heliyon.2020.e04201